Acta Crystallographica Section A
Foundations of Crystallography
ISSN 0108-7673

Received 4 May 2002
Accepted 24 June 2002

The best two-phase idealization of a sample in small-angle scattering

Salvino Ciccariello

Dipartimento di Fisica 'G. Galilei' e unità INFM, via Marzolo 8, I-35131 Padova, Italy.
Correspondence e-mail: ciccariello@pd.infn.it

The equations to be solved in order to determine the best discrete-valued approximation to a given electron or scattering-length density function are worked out. A simple illustration is reported.

The theory of small-angle scattering (SAS) of X-rays and neutrons (Guinier & Fournet, 1955; Glatter & Kratky, 1982; Feigin & Svergun, 1987; Kostorz, 1996) is based on the assumption that $n(\mathbf{r})$, the electron or the scattering-length density [simply referred to in the following as scattering density (function)] of the sample under analysis can fairly be approximated by a discrete-valued function denoted by $n_D(\mathbf{r})$ (Debye *et al.*, 1957; Porod, 1951; Ciccariello *et al.*, 1988). However, to the author's knowledge, the procedure able to determine $n_D(\mathbf{r})$ from $n(\mathbf{r})$, assumed to be known, was nowhere discussed. The aim of this note is to fill this gap in the simplest case of samples idealized as consisting of two homogeneous phases. In this case, $n_D(\mathbf{r})$ takes only two values, respectively denoted by n_1 and n_2. The hypothetical sample with scattering density $n_D(\mathbf{r})$ will be called the Debye idealized sample. Denote by $\mathcal{V}_1$ and $\mathcal{V}_2$ the collection of the regions of the Debye sample where $n_D(\mathbf{r})$ is equal to n_1 and to n_2, respectively. The two regions are fully determined by their *set characteristic functions* $\rho_1(\mathbf{r})$ and $\rho_2(\mathbf{r})$. It is recalled that $\rho_j(\mathbf{r})$ (with $j = 1, 2$) is defined as being equal to one if the tip of the position vector $\mathbf{r}$ lies inside $\mathcal{V}_j$ and equal to zero elsewhere. Denoting the set characteristic function of the sample by $\rho_V(\mathbf{r})$, one finds that

$$\rho_1(\mathbf{r}) + \rho_2(\mathbf{r}) = \rho_V(\mathbf{r}) \tag{1}$$

and

$$n_D(\mathbf{r}) = n_1\rho_1(\mathbf{r}) + n_2\rho_2(\mathbf{r}) = \Delta n\rho_1(\mathbf{r}) + n_2\rho_V(\mathbf{r}), \tag{2}$$

where $\Delta n \equiv (n_1 - n_2)$ is the scattering contrast between the two phases constituting the Debye sample.

It appears natural to require that the best discrete-valued approximation of $n(\mathbf{r})$ is the function $n_D(\mathbf{r})$ which makes the integral

$$\mathcal{I} \equiv \int_V |n(\mathbf{r}) - n_D(\mathbf{r})|^2 \, \mathrm{d}v \tag{3}$$

smallest. [The integral in (3) is performed throughout the sample volume denoted by V.] Recalling that $\nu_D(\mathbf{r}) \equiv [n(\mathbf{r}) - n_D(\mathbf{r})]$ represents the microscopic fluctuation of the density of the given sample in comparison to that of the Debye one, then $\mathcal{I}$ represents the squared L_2 norm of $\nu_D(\mathbf{r})$. Thus, minimizing $\mathcal{I}$ amounts to making $\nu_D(\mathbf{r})$ smallest in norm.[1]

To show how to get the equations that determine the best $n_D(\mathbf{r})$, consider first the simplest case where the idealized sample consists of a smooth, convex and homogeneous particle that is immersed in a homogeneous medium. This implies that the particle surface, denoted by Σ, does not present edges and corner points and that each segment having its two ends on Σ has the remaining points inside the particle. Let $\mathbf{r}_G$ denote the position vector of the centre of gravity of the particle and consider a new Cartesian frame $O'x'y'z'$, having the origin at the particle's centre of gravity, so as to have

$$\mathbf{r} = \mathbf{r}_G + \mathbf{r}'. \tag{4}$$

The particle's set characteristic function, with respect to the $O'x'y'z'$ frame, will be denoted as $\rho_p(\mathbf{r}')$. It is related to $\rho_1(\mathbf{r})$ by the relation

$$\rho_p(\mathbf{r}') = \rho_1(\mathbf{r}' + \mathbf{r}_G). \tag{5}$$

Using polar coordinates (r', θ', φ') and putting $\hat{\mathbf{r}}' = (\cos(\varphi')\sin\theta', \sin(\varphi')\sin\theta', \cos\theta')$, we have $\mathbf{r}' = r'\hat{\mathbf{r}}'$. The convexity assumption implies that, along any direction $\hat{\mathbf{r}}'$,

$$\rho_p(\mathbf{r}') = \rho_p(r'\hat{\mathbf{r}}') = \Theta[R(\theta', \varphi') - r'], \tag{6}$$

where Θ is the Heaviside function and $R(\theta', \varphi')$ is the distance from the origin of the system $O'x'y'z'$ to the point intersection of Σ with the half straight line having direction $\hat{\mathbf{r}}'$ and passing through O'. The knowledge of $R(\theta', \varphi')$, for any (θ', φ'), fully determines $\rho_p(\mathbf{r}')$, *i.e.* the particle shape, while that of $\mathbf{r}_G$ determines the position of the particle in the space. Writing $n_D(\mathbf{r})$ as

$$n_D(\mathbf{r}) = \Delta n\rho_1(\mathbf{r}) + n_2\rho_V(\mathbf{r}) = \Delta n\rho_p(\mathbf{r} - \mathbf{r}_G) + n_2\rho_V(\mathbf{r}), \tag{7}$$

[1] This condition can also be restated by saying that the best $n_D(\mathbf{r})$ minimizes the integral, over reciprocal space, of the scattering intensity $[I_{\mathrm{mfl}}(\mathbf{q})]$ of a hypothetical sample having its scattering density equal to $\nu_D(\mathbf{r})$. In fact, denoting the Fourier transform of a function by the same symbol with a tilde, the Parseval equality allows us to write (3) as $\mathcal{I} = (1/2\pi)^3 \int |\tilde{\nu}_D(\mathbf{q})|^2 \, \mathrm{d}v_q = (1/2\pi)^3 \int I_{\mathrm{mfl}}(\mathbf{q}) \, \mathrm{d}v_q$.

one concludes that $n_D(\mathbf{r})$ is fully known once $\rho_p(\mathbf{r}')$, $\mathbf{r}_G$, Δn and n_2 have been determined. It remains to be shown how these quantities can be determined by making $\mathcal{I}$ minimum. For this condition to hold, the derivatives of $\mathcal{I}$ with respect to Δn, n_2, $\mathbf{r}_G$ and $R(\theta, \varphi)$ must be equal to zero. To evaluate these derivatives, it is first observed that (3) can be written by (4)–(7) as

$$\mathcal{I} = (\Delta n)^2 V_1 + n_2^2 V + 2n_2[(\Delta n)V_1 - V\langle n\rangle] + \int_V [n^2(\mathbf{r}) - 2(\Delta n)n(\mathbf{r})\rho_1(\mathbf{r})]\,\mathrm{d}v, \tag{8}$$

where $\langle n\rangle$ is the scattering density average of the real sample, *i.e.*

$$\langle n\rangle \equiv (1/V)\int_V n(\mathbf{r})\,\mathrm{d}v, \tag{9}$$

and the particle volume V_1 as

$$V_1 = \int \rho_1(\mathbf{r})\,\mathrm{d}v = \iiint r'^2 \sin(\theta')\Theta[R(\theta', \varphi') - r']\,\mathrm{d}r'\,\mathrm{d}\theta'\,\mathrm{d}\varphi'. \tag{10}$$

One similarly shows that

$$\int n(\mathbf{r})\rho_1(\mathbf{r})\,\mathrm{d}v = \iiint r'^2 \sin(\theta')n(\mathbf{r}_G + r'\hat{\mathbf{r}}'(\theta', \varphi')) \times \Theta(R(\theta', \varphi') - r')\,\mathrm{d}r'\,\mathrm{d}\theta'\,\mathrm{d}\varphi', \tag{11}$$

which is the only contribution on the right-hand side (r.h.s.) of (8) depending on $\mathbf{r}_G$. Then from (8) it follows that

$$\partial\mathcal{I}/\partial\Delta n = 2[V_1\Delta n + V_1 n_2 - \int n(\mathbf{r})\rho_1(\mathbf{r})\,\mathrm{d}v], \tag{12a}$$

$$\partial\mathcal{I}/\partial n_2 = 2[V_1\Delta n + Vn_2 - V\langle n\rangle], \tag{12b}$$

$$\partial\mathcal{I}/\partial\mathbf{r}_{G,\alpha} = -2\Delta n \iiint r'^2 \sin(\theta')[\partial n(\mathbf{r}_G + r'\hat{\mathbf{r}}'(\theta', \varphi'))/\partial\mathbf{r}_{G,\alpha}] \times \Theta[R(\theta', \varphi') - r']\,\mathrm{d}r'\,\mathrm{d}\theta'\,\mathrm{d}\varphi', \tag{12c}$$

where $\mathbf{r}_{G,\alpha}$ is the αth component (with $\alpha = 1, 2, 3$) of $\mathbf{r}_G$. The derivative of $\mathcal{I}$ with respect to $R(\theta, \varphi)$ is a functional derivative that is evaluated by using the identity (Hansen & McDonald, 1976)

$$\delta R(\theta', \varphi')/\delta R(\theta, \varphi) = \delta(\theta - \theta')\delta(\varphi - \varphi'),$$

where the δ functions present on the r.h.s. are Dirac functions and the same rules valid for normal derivatives are applied. Thus, from (8) it follows that

$$\delta\mathcal{I}/\delta R(\theta, \varphi) = [(\Delta n)^2 + 2n_2\Delta n][\delta V_1/\delta R(\theta, \varphi)] - 2\Delta n[\delta\textstyle\int n(\mathbf{r})\rho_1(\mathbf{r})\,\mathrm{d}v]/\delta R(\theta, \varphi), \tag{12d}$$

and from (10) and (11), *via* the reported identity, one gets

$$\delta V_1/\delta R(\theta, \varphi) = R^2(\theta, \varphi)\sin(\theta),$$

$$[\delta\textstyle\int n(\mathbf{r})\rho_1(\mathbf{r})\,\mathrm{d}v]/\delta R(\theta, \varphi) = R^2(\theta, \varphi)n(\mathbf{r}_G + R(\theta, \varphi)\hat{\mathbf{r}}(\theta, \varphi))\sin(\theta).$$

Collecting the previous results, one finds the equations that determine the solution of our problem, namely

$$V_1\Delta n + V_1 n_2 = \int n(\mathbf{r})\rho_1(\mathbf{r})\,\mathrm{d}v, \tag{13a}$$

$$V_1\Delta n + Vn_2 = V\langle n\rangle, \tag{13b}$$

$$n(\mathbf{r}_G + R(\theta, \varphi)\hat{\mathbf{r}}(\theta, \varphi)) = (\Delta n + 2n_2)/2, \tag{13c}$$

$$\iiint r'^2 \sin(\theta')\nabla_G n(\mathbf{r}_G + r'\hat{\mathbf{r}}(\theta', \varphi'))\Theta(R(\theta', \varphi') - r')\,\mathrm{d}r'\,\mathrm{d}\theta'\,\mathrm{d}\varphi' = 0. \tag{13d}$$

Equations (13*a*)–(13*c*) can be written in a more compact form. In fact, after putting

$$\langle n\rangle_1 \equiv (1/V_1)\int n(\mathbf{r})\rho_1(\mathbf{r})\,\mathrm{d}v = (1/V_1)\int_{V_1} n(\mathbf{r})\,\mathrm{d}v, \tag{14a}$$

$$\langle n\rangle_2 \equiv (1/V_2)\int n(\mathbf{r})\rho_2(\mathbf{r})\,\mathrm{d}v = (1/V_2)\int_{V_2} n(\mathbf{r})\,\mathrm{d}v, \tag{14b}$$

using (1) one finds that

$$V\langle n\rangle = V_1\langle n\rangle_1 + V_2\langle n\rangle_2. \tag{14c}$$

Equations (13*a*) and (13*b*), after being solved with respect to n_1 and n_2, yield

$$n_1 = \langle n\rangle_1 \tag{15a}$$

$$n_2 = \langle n\rangle_2, \tag{15b}$$

while (13*c*), owing to (15*a*) and (15*b*), takes the form

$$n(\mathbf{r}) = (\langle n\rangle_1 + \langle n\rangle_2)/2. \tag{15c}$$

Actually, (15*c*) [together with definitions (14*a*) and (14*b*)] is the equation that determines the best discrete-valued approximation to $n(\mathbf{r})$. To show this, it is first remarked that equations (15*a*)–(15*c*) no longer require that the sample be made up of a single and strictly convex particle. In fact, they make sense for any two-valued discrete idealization. Moreover, they also apply to one-dimensional (1D) and two-dimensional (2D) samples, provided integrals (14*a*) and (14*b*), defining $\langle n\rangle_1$ and $\langle n\rangle_2$, are interpreted as 1D and 2D integrals. Second, it is observed that (15*a*) and (15*b*) imply that the values n_1 and n_2 of the sought for $n_D(\mathbf{r})$ solution must be equal to the mean values of $n(\mathbf{r})$, respectively evaluated over the regions $\mathcal{V}_1$ and $\mathcal{V}_2$ relevant to phases 1 and 2. Finally, according to (15*c*), the interface between phases 1 and 2 is the 'surface' where $n(\mathbf{r})$ turns out to be equal to the arithmetic mean of $\langle n\rangle_1$ and $\langle n\rangle_2$. Thus, (15*c*) determines the boundaries of the regions with scattering densities n_1 and n_2 as well as the latter values since the boundaries must be such that the mean values of $n(\mathbf{r})$, evaluated over the resulting $\mathcal{V}_1$ and $\mathcal{V}_2$ regions, must respectively be equal to n_1 and n_2.[2] These considerations show that the equation that really determines the Debye sample is (15*c*). In order to make fully clear how (15*c*) determines the best $n_D(\mathbf{r})$, consider the case of a 2D sample so that $n(\mathbf{r})$ is defined on a planar set $\mathcal{S}$ with area S. As $\mathbf{r}$ ranges throughout $\mathcal{S}$, the values taken by the continuous function $n(\mathbf{r})$ will range in an interval denoted by $[\Lambda_m, \Lambda_M]$. Further, the points $(\mathbf{r}, n(\mathbf{r}))$ define a surface with respect to a Cartesian frame $Oxyz$ such that $\mathcal{S}$ lies on the plane $z = 0$. Consider now the equation

$$n(\mathbf{r}) = \Lambda, \tag{16}$$

Λ being a real number such that $\Lambda_m \leq \Lambda \leq \Lambda_M$. The solution of (16) in general determines a curve, which will be first assumed to be a single closed curve, denoted by $\Gamma(\Lambda)$. This

[2] It should also be noted that (15*a*) and (15*b*) together with (14*c*) imply that $\langle n_D\rangle = \langle n\rangle$ so as to have $V\langle v_D\rangle = 0$ (Sobry & Ciccariello, 2002).

curve divides $\mathcal{S}$ in two disjoint sets: $\mathcal{S}_1(\Lambda)$, the region of $\mathcal{S}$ internal to $\Gamma(\Lambda)$, and $\mathcal{S}_2(\Lambda) = \mathcal{S} \setminus \mathcal{S}_1(\Lambda)$, the remaining region of $\mathcal{S}$, *i.e.* the region of $\mathcal{S}$ external to $\Gamma(\Lambda)$. For definiteness, assume that $n(\mathbf{r}) > \Lambda$ for all the vectors $\mathbf{r}$ whose tips lie inside $\mathcal{S}_1(\Lambda)$. This region will be identified with the region where $n_D(\mathbf{r}) = n_1$, so that $\rho_1(\mathbf{r}) = 1$ if $\mathbf{r} \in \mathcal{S}_1(\Lambda)$ and $\rho_1(\mathbf{r}) = 0$ if $\mathbf{r} \notin \mathcal{S}_1(\Lambda)$. The knowledge of $\rho_1(\mathbf{r})$ implies that of $\rho_2(\mathbf{r})$ by (1), and $\langle n\rangle_1$ and $\langle n\rangle_2$ can be respectively evaluated by (14*a*) and (14*b*). The resulting values depend on Λ and will be denoted as $\langle n\rangle_1(\Lambda)$ and $\langle n\rangle_2(\Lambda)$, respectively. Equation (15*c*) requires that their arithmetic mean be equal to Λ, the value taken by $n(\mathbf{r})$ on $\Gamma(\Lambda)$. This condition will be satisfied only for particular values of Λ. Thus, the solution of (15*c*) is obtained by looking at the intersection(s) of the curve $(\Lambda, [\langle n\rangle_1(\Lambda) + \langle n\rangle_2(\Lambda)]/2)$ with the straight line (Λ, Λ) as Λ ranges in $[\Lambda_m, \Lambda_M]$. This condition is clearly equivalent to looking for the solutions of the equation

$$[\langle n\rangle_1(\Lambda) + \langle n\rangle_2(\Lambda)]/2 - \Lambda = 0 \qquad (17)$$

within the range $\Lambda_m \leq \Lambda \leq \Lambda_M$, having clearly in mind that the evaluation of $\langle n\rangle_1(\Lambda)$ and $\langle n\rangle_2(\Lambda)$ requires the knowledge of $\mathcal{S}_1(\Lambda)$ and $\mathcal{S}_2(\Lambda)$ by solving (16) for each Λ value in $[\Lambda_m, \Lambda_M]$. Depending on whether an intersection exists or not, a Debye sample can or cannot be associated to the given sample. Assuming that the intersection occurs for the value $\bar{\Lambda}$ of Λ, the boundary of the two homogeneous phases is the curve $\Gamma(\bar{\Lambda})$ solution of the equation $n(\mathbf{r}) = \bar{\Lambda}$, while the scattering densities of the resulting homogeneous phases $\mathcal{S}_1(\bar{\Lambda})$ and $\mathcal{S}_2(\bar{\Lambda})$, defined by $\Gamma(\bar{\Lambda})$, are $\langle n\rangle_1(\bar{\Lambda})$ and $\langle n\rangle_2(\bar{\Lambda})$, respectively. It could also happen that (17) has more than one solution. In such a case, the best discrete-valued function is the solution that yields the minimum value of $\mathcal{I}$.

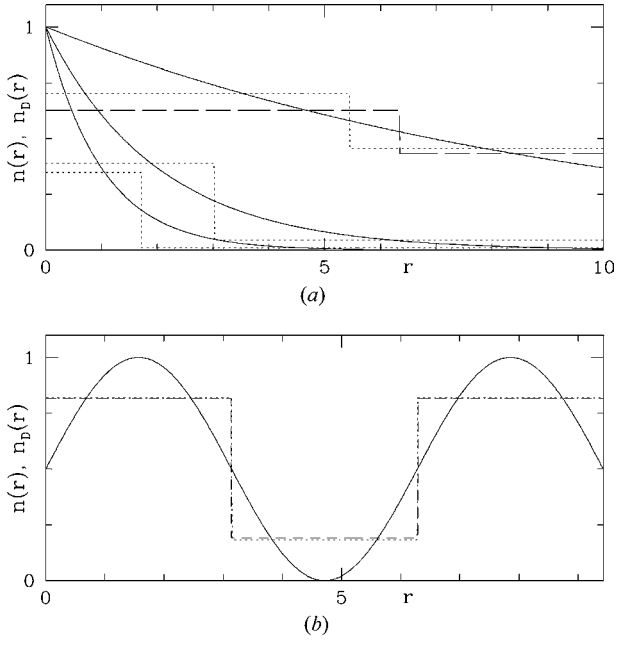

Figure 1
(*a*) The continuous lines show the profiles of the radially symmetric 'real' scattering density $n(\mathbf{r}) = \exp(-\lambda r)$ with $\lambda = 0.1$, 0.5 and 1, from top to bottom. The dotted lines show the profiles of the corresponding best $n_D(\mathbf{r})$ for the 2D case, while the broken line is the profile of the best two-phase idealization for $\lambda = 0.1$ in the 3D case. (*b*) The continuous line represents the profile of the radial 'real' scattering density $n(\mathbf{r}) = [1 + \sin(r)]/2$. The dotted and the broken curves, almost coinciding, represent the corresponding Debye approximations obtained by solving (15*c*) in the 2D and 3D case, respectively.

Whenever the solution of (16) consists of more closed curves (taking also into account the boundary of the sample), the separation of $\mathcal{S}$ into two disjoint sets $\mathcal{S}_1(\Lambda)$ and $\mathcal{S}_2(\Lambda)$ is performed by looking at the regions where $n(\mathbf{r}) > \Lambda$ and the regions where $n(\mathbf{r}) < \Lambda$. To the first regions will be assigned the value $n_1 = \langle n\rangle_1(\Lambda)$, and to the second the value $n_2 = \langle n\rangle_2(\Lambda)$, with $n_1 > n_2$. Each of the regions, forming the sets $\mathcal{S}_1(\Lambda)$ and $\mathcal{S}_2(\Lambda)$, is bounded by one or two of the aforesaid closed curves. Thus, the search of the Λ value, solution of (17), proceeds as in the above discussed case, even though the search of the solution is more complicated since an accurate book-keeping of all the regions is required. Finally, the previous considerations immediately generalize to the three-dimensional (3D) case. From this analysis, it follows that (15*c*) fully determines $\rho_1(\mathbf{r})$ and $\rho_2(\mathbf{r})$ and it becomes evident that the use of (13*d*) is no longer necessary. In fact, one can show that, for each particle, (13*d*) can be converted into $\mathbf{r}_G = (1/V_p)\int_V \mathbf{r}\rho_p(\mathbf{r})\,\mathrm{d}v$, *i.e.* the definition of the position of the centre of gravity of the particle.

A very simple illustration of the aforesaid procedure is shown in Figs. 1(*a*) and (*b*), which respectively illustrate the results obtained by considering the radially symmetric density profiles $n(\mathbf{r}) = \exp(-\lambda r)$ with $0 \leq r = |\mathbf{r}| \leq 10$ and $n(\mathbf{r}) = [1 + \sin(r)]/2$ with $0 \leq r \leq 3\pi$. In both cases, the radial symmetry makes it evident that the roots of the equation $n(\mathbf{r}) = \Lambda$ are circles or spheres, depending on whether one considers the 2D or the 3D case, so that the solutions of the equation $n(\mathbf{r}) = \Lambda$ yield their radii. For the profiles of Fig. 1(*a*), one finds that the radius, in terms of Λ, is $-\ln(\Lambda)/\lambda$. The evaluation of $\langle n\rangle_1(\Lambda)$ and $\langle n\rangle_2(\Lambda)$ can algebraically be carried through both in the 2D and in the 3D case, and the resulting equation (17) is easily solved numerically. In Fig. 1(*a*), the continuous lines show the 'real' profiles for $\lambda = 0.1$, 0.5 and 1 going from the top to the bottom, the dotted lines represent the profiles of the corresponding best two-phase idealizations for the 2D case and, finally, the broken line shows the profile of the best two-phase idealization of the real profile with $\lambda = 0.1$ for the 3D case. For the real profile shown in Fig. 1(*b*), one finds that $\Lambda_m = 0$, $\Lambda_M = 1$, while the roots of the equations $n(r) = \Lambda$ are $r(\Lambda) = \arcsin(2\Lambda - 1)\,(\equiv 2\pi)$ and $\pi - r(\Lambda)\,(\equiv 2\pi)$. In the two-dimensional case, both $\mathcal{S}_1(\Lambda)$ and $\mathcal{S}_2(\Lambda)$ consist of circular annuli (reducing to a circle when the inner radius is zero) with radii equal to the next-neighbour values among the set of the aforesaid values (including also the values 0 and 3π), which do not exceed 3π. Also for this 'real' profile, the evaluation of $\langle n\rangle_1(\Lambda)$ and $\langle n\rangle_2(\Lambda)$ is straightforward and the search of the root of (17) is made by numerically exploring the range $0 \leq \Lambda \leq 1$. The radial profile of the resulting $n_D(\mathbf{r})$ is given by the dotted line in Fig. 1(*b*). The analysis in the 3D case is quite similar since

$\mathcal{S}_1(\Lambda)$ and $\mathcal{S}_2(\Lambda)$ consist now of hollow spheres. The corresponding best $n_D(\mathbf{r})$ profile is given by the broken curve which is quite close to the dotted one.

Summarizing, the best discrete-valued approximation $n_D(\mathbf{r})$ to a given scattering-density function $n(\mathbf{r})$ is obtained by solving (15*c*) and, whenever this equation has more than one solution, by selecting the solution that makes $\mathcal{I}$ minimum. Even though this result can hardly be useful on practical grounds because of the mathematical difficulty of solving (15*c*) and, more important, because $n(\mathbf{r})$ is generally unknown, it is theoretically valuable. In fact, it shows that $n_D(\mathbf{r})$ turns out to be uniquely determined by the condition that $\mathcal{I}$ be minimum (barring the exceptional case of a degenerate minimum), it gives a procedure for determining $n_D(\mathbf{r})$ and, finally, it shows that the idealized interface is made up of the points where $n(\mathbf{r}) = (n_1 + n_2)/2$.

References

Ciccariello, S., Goodisman, J. & Brumberger, H. (1988). *J. Appl. Cryst.* **21**, 117–128.

Debye, P., Anderson, H. R. & Brumberger, H. (1957). *J. Appl. Phys.* **28**, 679–683.

Feigin, L. A. & Svergun, D. I. (1987). *Structure Analysis by Small-Angle X-ray and Neutron Scattering.* New York: Plenum Press.

Glatter, O. & Kratky, O. (1982). *Small-Angle X-ray Scattering.* London: Academic Press.

Guinier, A. & Fournet, G. (1955). *Small-Angle Scattering of X-rays.* New York: Wiley.

Hansen, J. P. & McDonald, I. R. (1976). *Theory of Simple Liquids*, Section 4.2. London: Academic Press.

Kostorz, G. (1996). *Physical Metallurgy*, edited by R. W. Cahn & P. Haasen, Vol. I, ch. 12. Amsterdam: North-Holland.

Porod, G. (1951). *Kolloid Z.*, **125**, 109–122.

Sobry, R. & Ciccariello, S. (2002). *J. Appl. Cryst.* **35**, 220–227.